

Article

Dynamical Analysis and Adaptive Finite-Time Sliding Mode Control Approach of the Financial Fractional-Order Chaotic System

Muhamad Deni Johansyah ^{1,*}, Aceng Sambas ², Saleh Mobayen ^{3,4}, Behrouz Vaseghi ⁵,
Saad Fawzi Al-Azzawi ⁶, Sukono ¹ and Ibrahim Mohammed Sulaiman ⁷

¹ Department of Mathematics, Universitas Padjadjaran, Sumedang 45363, Indonesia

² Department of Mechanical Engineering, Universitas Muhammadiyah Tasikmalaya, Tasikmalaya 46196, Indonesia

³ Department of Electrical Engineering, Faculty of Engineering, University of Zanjan, Zanjan 45371, Iran

⁴ Graduate School of Intelligent Data Science, National Yunlin University of Science and Technology, 123 University Road, Section 3, Douliou, Yunlin 640301, Taiwan

⁵ Department of Electrical and Computer Engineering, Abhar Branch, Islamic Azad University, Abhar 6134937333, Iran

⁶ Department of Mathematics, University of Mosul, Mosul 00964, Iraq

⁷ School of Quantitative Sciences, Universiti Utara Malaysia, Sintok 06010, Malaysia

* Correspondence: muhamad.deni@unpad.ac.id

Abstract: In this work, we studied the complex behaviors of the fractional-order financial chaotic system, consisting of a simple, relatively chaotic system with two quadratic nonlinearities (QN) and a sextic nonlinearity (SN). We completed and enriched the results presented in the study of Subartini et al. (2021). As a result of this, our study focused more on the fractional order and adaptive finite-time sliding mode control in the financial risk chaotic system. The dynamical behaviors of the financial chaotic system (FCS) with two QN and an SN were analyzed, and the stability was investigated via the Cardano method. The stability analysis showed that the real part of all the roots was negative, which confirmed the stability of the new system under the typical parameters. By using the MATLAB simulation, these properties were characterized, including the phase portraits, 0-1 test, Poincaré map, bifurcation diagram, and Lyapunov exponent. The analysis showed that the financial risk chaotic system of fractional order was able to exhibit chaotic behavior and periodical behavior. In spite of external perturbations and uncertainty, an adaptive finite-time sliding mode control strategy was devised to guide the states of the financial chaotic system to the origin in a finite amount of time. MATLAB phase plots were employed in this study to illustrate all the main results.

Keywords: chaos; fractional-order system; bifurcation; financial chaotic system (FCS); adaptive control

MSC: 65P20; 26A33; 34A34; 65L07; 65L06; 93C40



Citation: Johansyah, M.D.; Sambas, A.; Mobayen, S.; Vaseghi, B.; Al-Azzawi, S.F.; Sukono; Sulaiman, I.M. Dynamical Analysis and Adaptive Finite-Time Sliding Mode Control Approach of the Financial Fractional-Order Chaotic System. *Mathematics* **2023**, *11*, 100. <https://doi.org/10.3390/math11010100>

Academic Editor: Daniel-Ioan Curiaç

Received: 21 November 2022

Revised: 19 December 2022

Accepted: 22 December 2022

Published: 26 December 2022



Copyright: © 2022 by the authors. Licensee MDPI, Basel, Switzerland. This article is an open access article distributed under the terms and conditions of the Creative Commons Attribution (CC BY) license (<https://creativecommons.org/licenses/by/4.0/>).

1. Introduction

In many complex systems in several domains, chaos is a complex, nonlinear, dynamic process, such as in magnetic levitation [1], aerodynamic models of wind turbines [2], radar communication systems [3], encryption [4], electronic circuits [5], quarter-car vehicle models [6], ground vehicle oscillating systems with passengers [7], bimolecular chemical reaction–diffusion models [8], Aihara neuron networks [9], Field-Programmable Gate Arrays [10], mobile robots [11], financial models [12], and psychological stress [13]. In recent years, various applications of chaotic systems in the financial system have intensively been studied, such as the IS-LM model with distributed tax collection lags [14], the business

cycle model by Kaldor [15], New Keynesian macroeconomics [16], US inflation, and commodity prices [17]. This phenomenon makes it possible to determine the chaotic behavior of changes in interest rates, investment demands, and the prices of goods [18]. Specifically, market environment uncertainties interfere with the financial system. As a result, using a dynamical complex to describe the financial chaos model is more practical.

One of the greatest differences between fractional-order and integer-order models is that fractional-order models depend on the history of the system, that is, they possess memory [19]. Financial variables, such as exchange rates, gross domestic product, interest rates, production, and stock prices, can have very long memory, that is, our past economic behavior can affect our present and future behaviors. This means that all the fluctuations in the financial variables correlate with all the future fluctuations. Thus, the fact that the economic variables possess long memory makes fractional calculus suitable for studying dynamic behaviors in economic systems.

Many fractional-order chaotic models for the financial chaotic system have been studied to investigate the complex behavior in the literature. Wang et al. [20] developed a novel finite-time process that controls and synchronizes a 4D fractional-order system with market assurance. Chen [21] investigated the financial system of fractional order with two quadratic nonlinearities; in addition, he demonstrated several dynamic behaviors of interest, including chaotic motion, periodic motion, and fixed points. In [22], a complete and finite-time synchronization technique for the stabilization of fractional-order fuzzy neural network systems using the nonlinear feedback control approach was proposed. Without transforming the quaternion-valued neural networks into equivalent complex-valued systems, the global synchronization of fractional-order quaternion-valued neural network systems were studied in [23]. The complexity of a financial system of fractional order with a time delay has been examined by Wang et al. [24]. It was discovered that chaos and many other states might be observed with various parameters. In order to reduce the risk and unpredictable nature of financial decisions, Pan et al. [25] investigated the efficacy of adopting fuzzy control methods of fractional order for chaos suppression in a financial system with two QNs. A novel fractional-order finance system with negative values for the system's parameters was presented by Tacha et al. [26]. They demonstrated how these findings may be relevant to the study of economies that are negatively impacted, such as those that experience dissaving during a financial crisis. Hajipour and Tavakoli [27] introduced another chaotic system of fractional order with one quadratic nonlinearity and one absolute nonlinearity. They illustrated the system's chaotic behaviors by assuming lower values for the savings amount or cost per investment variable, or higher values for the elasticity of demand of commercial markets. Yousri and Mirjalili [28] defined a method to examine the corresponding parameters of fractional-order chaotic dynamical behavior for a hyperchaotic financial system. Cao [29] investigated the coupled synchronous control method with the aim of synchronizing a fractionally ordered chaotic financial system, while Wang [30] identified and predicted the symmetric chaotic financial systems' nonlinear fractional order via neural networks, Gaussian process regression, and the Differential Evolution algorithm. To the best of our knowledge, there is no study available on the fractional-order financial chaotic system with two quadratic nonlinearities and a sextic nonlinearity based on the aforementioned literature. Motivated by the above discussion, chaos in the financial system presented by Subartini et al. [31] is investigated in the present study. The adaptive sliding mode control (ASMC) technique is a common robust control approach that has been used for the stabilization/synchronization of various chaotic systems, such as chaotic chain systems [32], fractional-order chaotic systems [33], chaotic gyros [34], the Genesio–Tesi chaotic system [35], fractional hyperchaotic systems [36], drive–response chaotic systems [37], memristor-based systems [38], the chaotic non-smooth-air-gap permanent magnet synchronous motor [39], time-delay chaotic systems [40], and power systems' chaotic oscillations [41], etc. The ASMC technique is designed based on sliding mode control (SMC) and adaptive switching gains. The adaptive switching gains are employed to regulate the robust gains of SMC online. This

approach not only reduces the chattering phenomenon effects, but it also deals with the time-varying exterior disturbances of the control system. In this work, we performed a stability and dynamical analysis for the fractional-order financial chaotic system using the phase portraits, 0-1 test, Poincaré map, Lyapunov exponent, and bifurcation diagram. Finally, the chaos in this fractional-order financial system was controlled by a finite-time sliding mode control law, which can operate with or without external disturbances and uncertainties.

The remaining part of the research is organized as follows: Section 2 deals with the mathematical models and dynamical analysis of the financial chaotic system. Section 3 elaborates upon the dynamical behavior and mathematical model of the financial chaotic system in fractional order. In Section 4, a numerical simulation of the finite-time SMC law is described, and the conclusion is presented in Section 5.

2. Mathematical Models of the Financial Chaotic System

In 2021, Subartini et al. [31] defined a new financial chaotic system as follows:

$$\begin{cases} \dot{x} = z + (y - a)x \\ \dot{y} = 1 - b(y + x^2) - cx^6 \\ \dot{z} = -x - z \end{cases} \tag{1}$$

Based on the above system, this study will show that for the following parameter values:

$$a = 7.6, b = 0.1, c = 0.2 \tag{2}$$

the system (1) will exhibit a chaotic attractor.

The following initial conditions will be considered in numerical simulations:

$$x(0) = 0.4, y(0) = 0.2, \text{ and } z(0) = 0.5 \tag{3}$$

Using the linear approximation method on the proposed system, the characteristic equation becomes:

$$\lambda^3 + \underbrace{(ab + 1)}_{C_1}\lambda^2 + \underbrace{(a + b + ab + 1)}_{C_2}\lambda + \underbrace{b(a + 1)}_{C_3} = 0 \tag{4}$$

According to Cardano’s Formula [42–44], the discriminant (Δ) for the above general cubic can be obtained as follows:

$$\Delta = -27C_3^2 - 4C_2^3 + 18 C_1C_2C_3 + C_1^2C_2^2 - 4C_1^3C_3 \tag{5}$$

The sign of the discriminant (Δ) is very significant in determining the type of root; the potential cases of the roots with the variety discriminant are given by:

$$\text{roots} = \begin{cases} \lambda_1, \lambda_{2,3} = a_i \pm b_i i ; & \text{if } \Delta > 0 \\ \lambda_1, \lambda_2 = \lambda_3 ; & \text{if } \Delta = 0 \\ \lambda_1 \neq \lambda_2 \neq \lambda_3 ; & \text{if } \Delta < 0 \end{cases} \tag{6}$$

whereas the corresponding roots for each discriminant are given in Formulas (7)–(9), respectively, as:

$$\lambda_1 = -2\sqrt[3]{\frac{h}{2}} - \frac{C_1}{3}, \quad \lambda_{2,3} = \sqrt[3]{\frac{h}{2}} - \frac{C_1}{3} \tag{7}$$

$$\lambda_{n+1} = \sqrt[6]{16(h^2 - \Delta)} \cos \frac{\cos^{-1} \frac{-h}{\sqrt{h^2 - \Delta}} + 2\pi n}{3} - \frac{C_1}{3} \quad n = 0, 1, 2. \tag{8}$$

$$\begin{cases} \lambda_1 = \sqrt[3]{\frac{-h-\sqrt{\Delta}}{2}} + \sqrt[3]{\frac{-h+\sqrt{\Delta}}{2}} - \frac{C_1}{3} \\ \lambda_{2,3} = -\frac{1}{2} \left(\sqrt[3]{\frac{-h-\sqrt{\Delta}}{2}} + \sqrt[3]{\frac{-h+\sqrt{\Delta}}{2}} \right) - \frac{C_1}{3} \pm i \frac{\sqrt{3}}{2} \left(\sqrt[3]{\frac{-h-\sqrt{\Delta}}{2}} - \sqrt[3]{\frac{-h+\sqrt{\Delta}}{2}} \right) \end{cases} \quad (9)$$

in which $h = C_3 - \frac{1}{3}C_1C_2 + \frac{2}{27}C_1^3$.

In order to simplify our results, we chose the parameter to be $(a, b, c) = (7.6, 0.1, 0.2)$, and relying on Cardano’s formula, we obtained $\Delta = -88.0026852$ and $h = 22.204$, and the values given in Table 1 are the corresponding roots.

Table 1. The roots of the proposed system obtained via Cardano’s formula.

Iteration	λ_1	λ_2	λ_3
$n = 0$	-0.1		
$n = 1$		-7.4448	
$n = 2$			-1.1552

Clearly, from Table 1, the real part of the roots are negative, which means that the new system is stable under the typical parameters. The signal plots of the financial system (1) with initial state $Y(0) = (0.4, 0.2, 0.5)$ and constant parameters $(a, b, c) = (7.6, 0.1, 0.2)$ (chaotic case) are simulated in Figure 1.

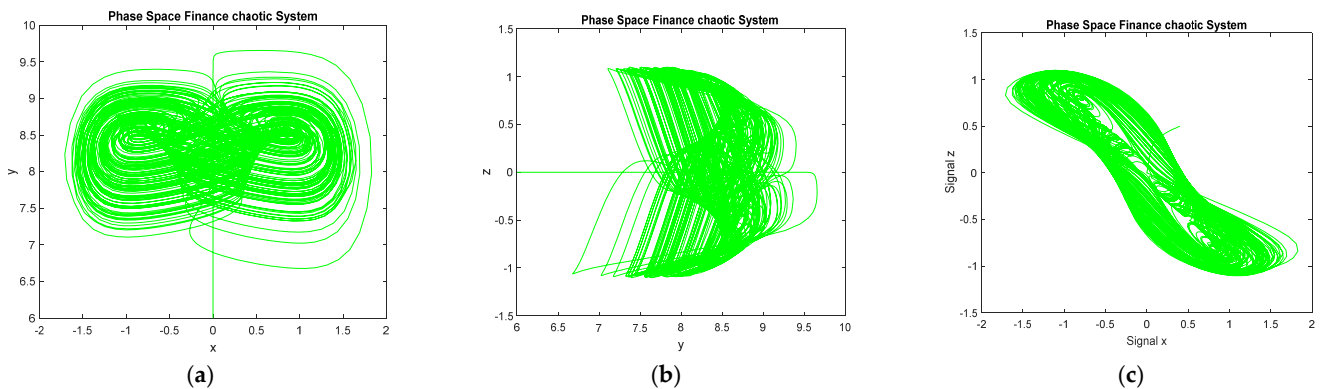


Figure 1. Output MATLAB simulation of the financial chaotic system (1) with $Y(0) = (0.4, 0.2, 0.5)$ and $(a, b, c) = (7.6, 0.1, 0.2)$: (a) x - y plane, (b) y - z plane, and (c) x - z plane.

The 0-1 test is an effective tool to determine whether the system is in a chaotic state [45]. The regular graph on the p - s plane indicates that the system is in a periodic or quasiperiodic state. Conversely, irregular graphics indicate that the system is in a state of chaos. However, if the system diverges, there will be no graphics on the p - s plane. Figure 2a displays the results of the 0-1 test with irregular graphics. Thus, in this case, the system shows chaotic behavior.

The Poincaré map is used to analyzed the motion characteristics of the multivariable autonomous system [45]. The phase diagram of the Poincaré map well characterizes the reciprocating non-periodic characteristics of chaos. If the Poincaré map is neither a finite set nor a closed curve, then the corresponding system’s motion is in a chaotic motion state. More specifically, if the system does not experience external noise disturbance and there is certain damping, then the Poincaré map will be a point set with a detailed structure. Moreover, if the Poincaré map is a finite set of a point, then the corresponding system motion is periodic. The Poincaré map of system (1) in Figure 2b likewise exhibits chaotic characteristics.

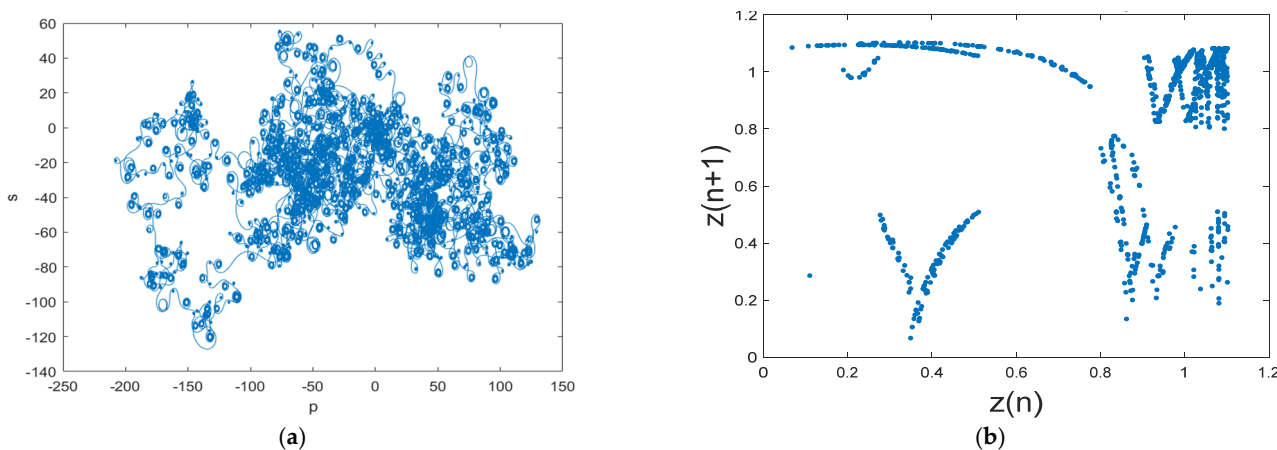


Figure 2. Output MATLAB simulation of the financial chaotic system (1) with $Y(0) = (0.4, 0.2, 0.5)$ and $(a, b, c) = (7.6, 0.1, 0.2)$: (a) x - y plane, and (b) Poincaré section of the financial chaotic system (1).

3. Mathematical Model of Fractional-Order Financial Chaotic System

Utilizing the Caputo definition, we have:

$$D^q f = \frac{1}{\Gamma(n-q)} \int_0^t (t-\tau)^{n-q-1} f^{(n)}(\tau) d\tau \quad (m-1 < q < m) \tag{10}$$

$$D^q f = \frac{d^n}{dt^n} f(t) \quad (q = n)$$

where Γ is the gamma function, and m is the lowest integer less than q , with q denoting the order of fractional derivatives. Here,

$$\Gamma(x) = \int_0^\infty t^{x-1} e^{-t} dt \tag{11}$$

The equivalent fractional-order model for system (1) can be mathematically described as follows:

$$\begin{cases} *D_{t_0}^q x = z + (y - a)x \\ *D_{t_0}^q y = 1 - b(y + x^2) - cx^6 \\ *D_{t_0}^q z = -x - z \end{cases} \tag{12}$$

with a, b , and c denoting the system parameters, q ($0 < q \leq 1$) is the order of the fractional-order differential equation, and the state variables are denoted by x, y , and z .

In Figure 3, we present the phase portrait for financial system (12) of commensurate fractional-order q . Obviously, the fractional-order financial chaotic system (12) can generate chaotic attractors for $q = 0.98$. Moreover, Figure 4 show the phase portrait's periodic behavior for the financial system with $q = 0.90$.

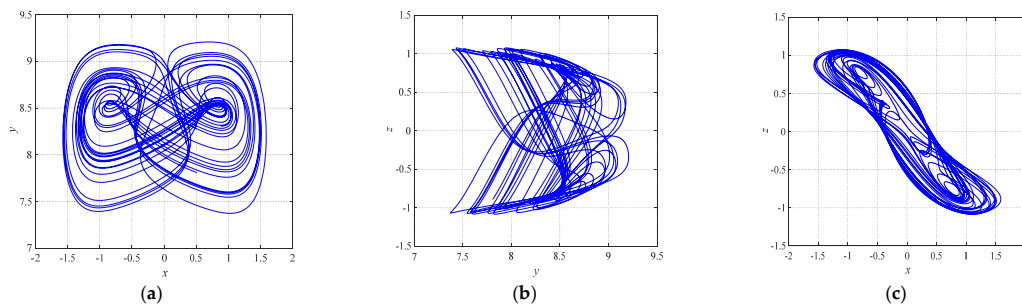


Figure 3. Phase diagrams for $q = 0.98$, $(a, b, c) = (7.6, 0.1, 0.2)$ with $x(0) = 0.4, y(0) = 0.2, z(0) = 0.5$: (a) x - y plane, (b) y - z plane, and (c) x - z plane.

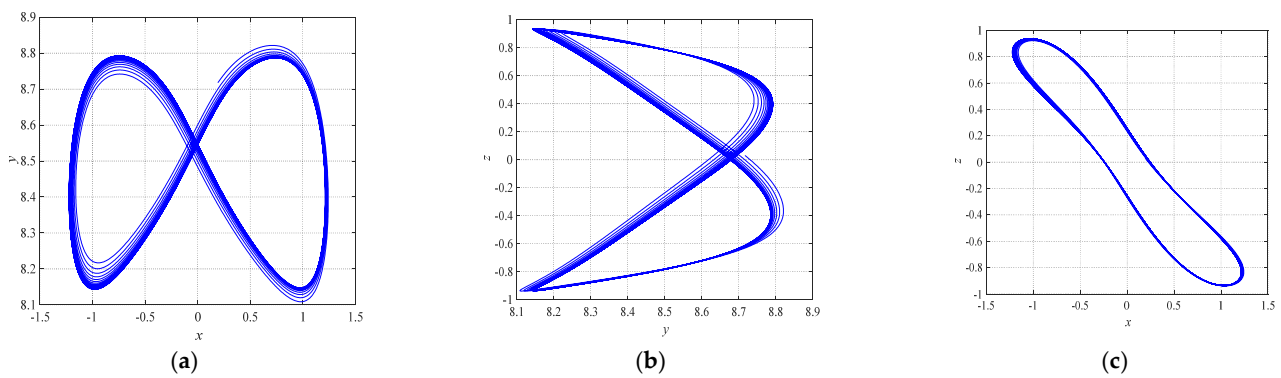


Figure 4. Phase diagrams for $q = 0.90$, $(a, b, c) = (7.6, 0.1, 0.2)$ with $x(0) = 0.4, y(0) = 0.2, z(0) = 0.5$: (a) x - y plane, (b) y - z plane, and (c) x - z plane.

In this work, the special-order q of the fractional financial chaotic system (12) has been used as a parameter to control the bifurcations and develop additional sophisticated dynamics. In this study, the Lyapunov exponent analysis was validated using the Wolf algorithm [46]. We set $(a, b, c) = (7.6, 0.1, 0.2)$, with $x(0) = 0.4, y(0) = 0.2$, and $z(0) = 0.5$. It is obvious from Figure 5 that the Lyapunov exponent spectrum coincides with the bifurcation diagram. Obviously, the fractional financial system (12) is able to display periodical and chaotic states.

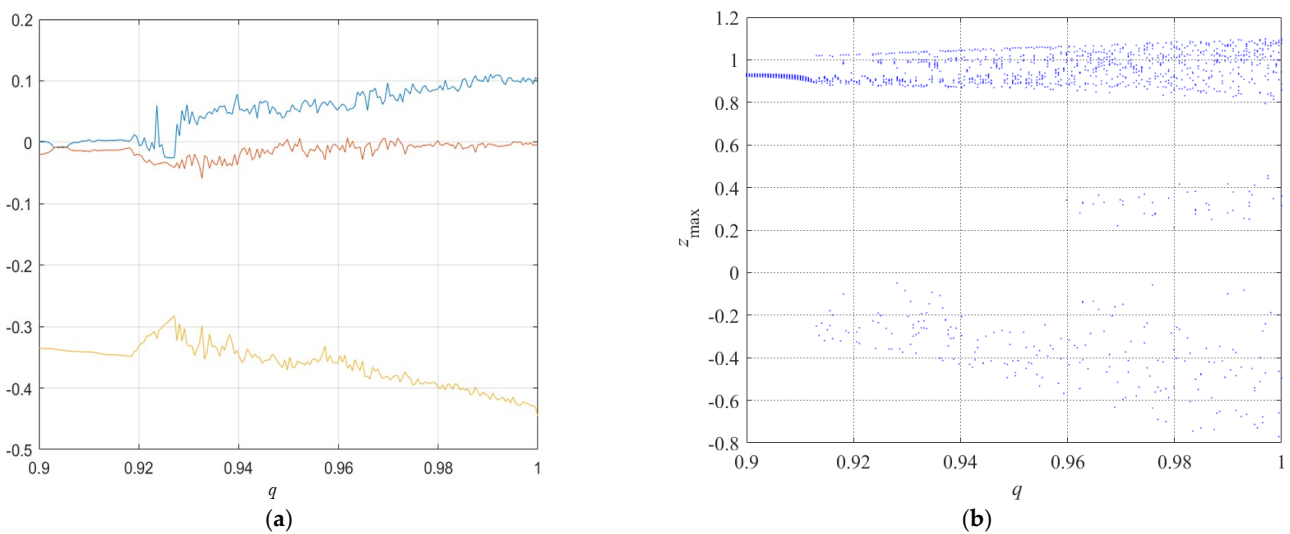


Figure 5. MATLAB simulation for financial fractional-order chaotic system: (a) Lyapunov exponent for $q [0.9 \ 1]$ and (b) bifurcation diagram for $q [0.9 \ 1]$.

4. Finite-Time Fast Synchronization

In this section, in order to transfer secure communication, we describe chaos control and finite-time fast synchronization.

4.1. Problem Formulation

Consider the new chaotic system (12). In order to achieve synchronization, we divided the new chaos system into two master–slave subsystems.

$$\left. \begin{aligned} \dot{x}_m &= z_m + (y_m - a)x_m \\ \dot{y}_m &= 1 - b(y_m + x_m^2) - cx_m^6 \\ \dot{z}_m &= -x_m - z_m \end{aligned} \right\} \text{Master subsystem} \tag{13}$$

$$\left. \begin{aligned} \dot{x}_s &= z_s + (y_s - a)x_s + D_1 + u_1 \\ \dot{y}_s &= 1 - b(y_s + x_s^2) - cx_s^6 + D_2 + u_2 \\ \dot{z}_s &= -x_s - z_s + D_3 + u_3 \end{aligned} \right\} \text{Slave subsystem}$$

where $v = [u_1 \ u_2 \ u_3]^T$ and $D = [D_1 \ D_2 \ D_3]^T$ are the control input and bounded uncertainties, respectively.

Assumption 1. In general, the synchronization of subsystems (13) is as follows:

$$(a_{si} - a_{mi})(\chi_{si} - \chi_{mi}) = a'_{i}e_i \quad i = 1, 2, 3 \tag{14}$$

Assumption 2. We will obtain fast finite-time synchronization between subsystems (13) if

$$\lim_{T \rightarrow \tau} \|e(T)\|, \|e(T)\| = 0 \text{ with } T \geq \tau, \text{ where } \tau = \tau(e(0)) > 0, e(T) = [(e_i)]^T \text{ for } i = 1, 2, 3 \tag{15}$$

Assumption 3. With $\chi_{si} = \chi_{mi}, i = 1, 2, 3$, the result is:

$$\lim_{T \rightarrow \infty} e_i(T) \quad i = 1, 2, 3 \tag{16}$$

The fast finite-time synchronization errors, due to Assumptions 1–3 and subsystems (13), are as follows:

$$\left\{ \begin{aligned} \dot{x}_s - \dot{x}_m &= z_s - z_m + (y_s - a_s)x_s - (y_m + a_m)x_m + D_1 + B_1u_1 \\ \dot{y}_s - \dot{y}_m &= 1 - b_s(y_s + x_s^2) + b_m(y_m + x_m^2) - cx_s^6 + cx_m^6 + D_2 + B_2u_2 \\ \dot{z}_s - \dot{z}_m &= -x_s + x_m - z_s + z_m + D_3 + B_3u_3 \end{aligned} \right. \quad (a_{si} - a_{mi})(\chi_{si} - \chi_{mi}) = a'_{i}e_i \tag{17}$$

$$\left\{ \begin{aligned} \dot{x}_s - \dot{x}_m &= \underbrace{(-a_s + a_m)}_{e_1}(x_s - x_m) + \underbrace{(z_s - z_m)}_{e_3} + \underbrace{(y_s x_s - y_m x_m)}_{f_1} + D_1 + B_1u_1 \\ \dot{y}_s - \dot{y}_m &= \underbrace{(-b_s + b_m)}_{e_2}(y_s - y_m) + \underbrace{(b_s x_s^2 - b_m x_m^2)}_{e_2} + \underbrace{(-c_s x_s^6 + c_m x_m^6)}_{f_2} + D_2 + B_2u_2 \\ \dot{z}_s - \dot{z}_m &= \underbrace{(-x_s + x_m)}_{e_3} + \underbrace{(-z_s + z_m)}_{-e_1} + \underbrace{D_3 + B_3u_3}_{-e_3} \end{aligned} \right. \tag{17}$$

In the matrix form,

$$\underbrace{\begin{bmatrix} \dot{e}_1 \\ \dot{e}_2 \\ \dot{e}_3 \end{bmatrix}}_{\dot{e}_i} = \underbrace{\begin{bmatrix} -a' & 0 & 1 \\ 0 & -b' & 0 \\ -1 & 0 & -1 \end{bmatrix}}_{\chi_i} \underbrace{\begin{bmatrix} e_1 \\ e_2 \\ e_3 \end{bmatrix}}_{e_i} + \underbrace{\begin{bmatrix} f_1 \\ f_2 \\ f_3 \end{bmatrix}}_{f_i} + \underbrace{[B_1 \ B_2 \ B_3]}_{B_i} \underbrace{\begin{bmatrix} u_1 \\ u_2 \\ u_3 \end{bmatrix}}_{v_i} + \underbrace{[\wp_1 \ \wp_2 \ \wp_3]}_{\wp_i} \underbrace{\begin{bmatrix} D_1 \\ D_2 \\ D_3 \end{bmatrix}}_{D_i} \quad i = 1, 2, 3 \tag{18}$$

where e_i is the error matrix, χ_i is the coefficient matrix, f_i is the nonlinear matrix, B_i is the controller coefficient, and φ_i is the uncertainty coefficient.

4.2. Adaptive Finite-Time Fast Terminal Sliding Mode Control Approach

According to system (18), the results are as follows:

$$\dot{e}_i = \chi_i e_i + f_i + B_i v_i + \varphi_i D_i \quad i = 1, 2, 3 \tag{19}$$

In system (19), the sliding surface is defined as follows:

$$l = \zeta e \tag{20}$$

where $\zeta = [\zeta_1 \ \zeta_2 \ \zeta_3]$ is the sliding manifold velocity vector. The fast finite-time sliding surface is given as:

$$\left. \begin{aligned} \delta &= e + \beta \delta_1 + l^{\mu_1/\mu_2} \\ \dot{\delta}_1 &= e + \gamma l^{\eta_1/\eta_2} \end{aligned} \right\} \text{fast finite-time sliding surface} \tag{21}$$

where $\delta_1(0) = -\beta^{-1}\delta(0)$, $\beta, \gamma > 0$ are positive constants. $\mu_1/\mu_2 > \eta_1/\eta_2$ are odd integers and $1 < \mu_1/\mu_2 < 2$. With $\delta = 0$, we obtain:

$$\dot{\delta}_1 = \left(-\beta \delta_1 - l^{\mu_1/\mu_2}\right) + \gamma \left(-\beta \delta_1 - l^{\mu_1/\mu_2}\right)^{\eta_1/\eta_2} \tag{22}$$

We define $K\Gamma = \beta \delta_1 + l^{\mu_1/\mu_2}$. Then, we obtain:

$$\dot{\delta}_1 = -K\Gamma - K^{\eta_1/\eta_2} \gamma \Gamma^{\eta_1/\eta_2} \tag{23}$$

Based on Euler–Bernoulli, we have:

$$\delta_1 = -K^{-1} e^{-K\Gamma} \left(-\gamma e^{K(1-\eta_1/\eta_2)\Gamma} + \beta^{1-\eta_1/\eta_2} \delta^{1-\eta_1/\eta_2}(0) + \gamma\right)^{\frac{1}{1-\eta_1/\eta_2}} \tag{24}$$

According to Equation (24), finite-time fast convergence is equal to:

$$T_s = \frac{1}{K(1-\eta_1/\eta_2)} \ln \frac{K^{1-\eta_1/\eta_2} |\delta_1(0)|^{1-\eta_1/\eta_2} + \gamma}{\gamma} = \frac{1}{K(1-\eta_1/\eta_2)} \ln \frac{|e(0)|^{1-\eta_1/\eta_2} + \gamma}{\gamma} \tag{25}$$

Theorem 1. Consider the nonlinear system (19). With sliding surface (21), we define the control input as follows:

$$v = B_i^{-1} \left\{ (\chi_i e_i + f_i - \text{sign}(\delta_i) \|\varphi_i\| D_{mi}) + \left(-\beta e_i - \beta \gamma e_i^{\eta_1/\eta_2} - \mu_1/\mu_2 l^{1-\mu_1/\mu_2} e_i\right) - \lambda \frac{\delta_i}{\|\delta_i\|} \right\} \tag{26}$$

where D_{mi} , $i = 1, 2, 3$ are the upper bounds of uncertainty and λ is the positive definite (pd) matrix and it is constant. By properly selecting the parameters defined in the newly designed controller, we will achieve fast finite-time convergence.

Proof. To validate the controller, let the function of the Lyapunov candidate be defined as follows:

$$v(t) = \frac{(\delta_i^T \delta_i)}{2} \tag{27}$$

The sliding surface δ derivative is obtained as follows:

$$\dot{\delta}_i = \dot{e}_i + \beta \dot{\delta}_1 + \mu_1/\mu_2 |l|^{\mu_1/\mu_2 - 1} \dot{l} \tag{28}$$

By placing (19) in (28), the result is:

$$\dot{\delta}_i = (\chi_i e_i + f_i + B_i v_i + \varphi_i D_i) + \beta (e + \gamma e^{\mu_1/\eta_2}) + \mu_1/\mu_2 |e|^{\mu_1/\mu_2 - 1} e \tag{29}$$

Substituting the new controller (26) into the derivative of the Lyapunov candidate function (27), the result is:

$$\begin{aligned} \dot{v}(t) &= \delta_i^T (\varphi_i D_i - \|\varphi_i\| \text{sign}(\delta_i) D_{mi} - \beta (e + \gamma e^{\mu_1/\eta_2}) - \mu_1/\mu_2 |e|^{1-\mu_1/\mu_2} e \\ &\quad - \lambda \frac{\delta_i}{\|\delta_i\|} + \beta \dot{\delta}_1 + \mu_1/\mu_2 |l|^{\mu_1/\mu_2 - 1} \dot{l}) \\ &= \delta_i^T \varphi_i D_i - \delta_i^T \|\delta_i\| \text{sign}(\delta_i) D_{mi} - \delta_i^T \lambda \frac{\delta_i}{\|\delta_i\|} \end{aligned} \tag{30}$$

We obtain:

$$\begin{aligned} &(\delta_i^T \varphi_i D_i - \|\delta_i\| \text{sign}(\delta_i) D_{mi}) \\ &= \sum_{i=1}^3 \delta_i \varphi_i D_i - \sum_{i=1}^3 |\delta_i| \varphi_i \text{sign}(\delta_i) D_{mi} \\ &\leq \sum_{i=1}^3 |\delta_i| |\varphi_i D_i| - \sum_{i=1}^3 |\delta_i| |\varphi_i| D_{im} \leq 0 \end{aligned} \tag{31}$$

By extending Equation (30) and according to Equation (31), the results are:

$$\begin{aligned} \dot{v}(t) &\leq -\delta_i^T \lambda \frac{\delta_i}{\|\delta_i\|} \\ &\leq -\sigma_{\min}(\lambda) \frac{\|\delta_i\|^2}{\|\delta_i\|} \\ &\leq -\sqrt{2} \sigma_{\min}(\lambda) v^{0.5}(t) \end{aligned} \tag{32}$$

Thus, it can be concluded that the sliding surface converges to the origin within a fast finite time. Convergence time is equal to:

$$T_s \leq \frac{v^{0.5}(\delta_i(t_0))}{\frac{1}{\sqrt{2} \sigma_{\min}(\lambda)}} = \frac{\|\delta_i(t_0)\|}{\sigma_{\min}(\lambda)} \tag{33}$$

The proof is complete. \square

4.3. Simulation Results of Adaptive Finite-Time Fast Terminal Sliding Mode Control

In this section, using MATLAB software, a simulation is described between two new nonlinear systems (13), with the new control system being defined in (26). By synchronizing these two systems, we achieve the goals of secure communication in a fast, finite timeframe.

The initial conditions and parameters of systems (13) are as follows:

$$\left. \begin{aligned} a_m = 7.6, b_m = 0.1, c_m = 0.2 \\ x_m(0) = 0.4, y_m(0) = 0.2, z_m(0) = 0.5 \end{aligned} \right\} \text{master values} \tag{34}$$

$$\left. \begin{aligned} a_s = 7.2, b_s = 0.16, c_s = 0.18 \\ x_s(0) = -1.5, y_s(0) = -1.33, z_s(0) = -1.78 \end{aligned} \right\} \text{slave values}$$

The controller parameters' numerical values are shown in Table 2.

Table 2. The controller values.

Parameter	Value
β	0.24
γ	0.036
μ_1	37
μ_2	11
η_1	21
η_2	9
λ	diag(0.5 1 1.5)
K	diag(0.57 0.29 0.06)
φ_i	[3.2 0.5 4.8]
B_i	[1 1 1]

The disturbances are given as:

$$D_i = \begin{bmatrix} 0.3 + 0.6 \sin(\omega t) \\ 0.8 - 0.7 \cos(2\omega t) \\ 0.4 - 0.9 \sin(1.2\omega t) \end{bmatrix} \tag{35}$$

Under the new controller (26), the complete synchronization and error synchronization of the nonlinear master–slave systems (13) are as presented in Figures 6–8. The controller input is shown in Figure 9.

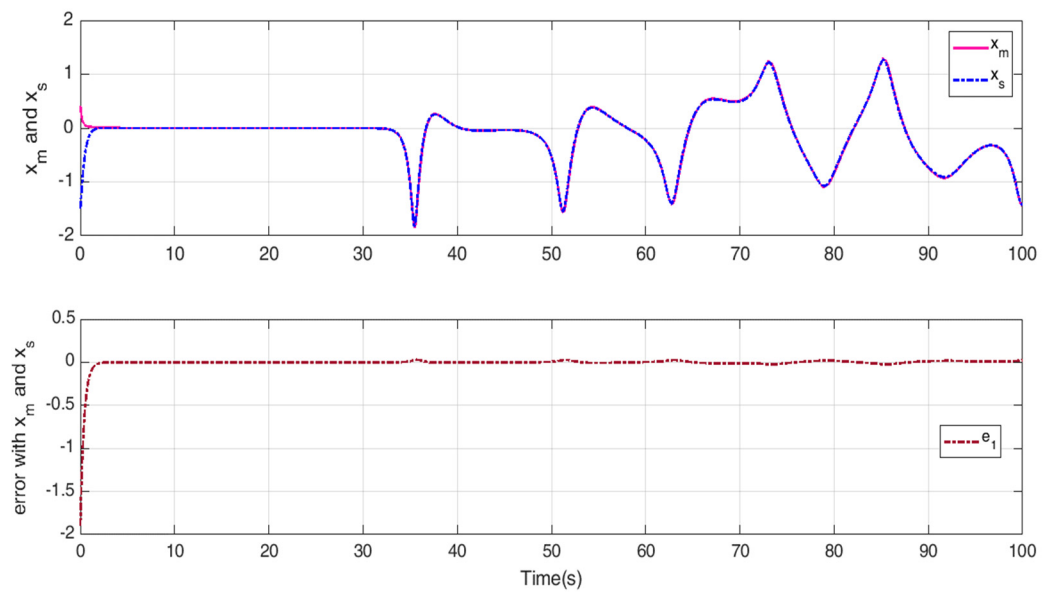


Figure 6. The master–slave synchronization of the first state.

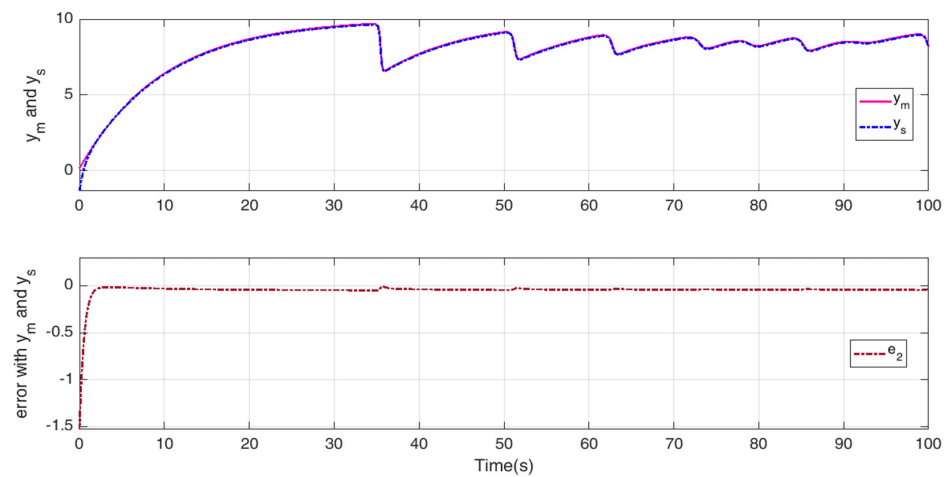


Figure 7. The master–slave synchronization of the second state.

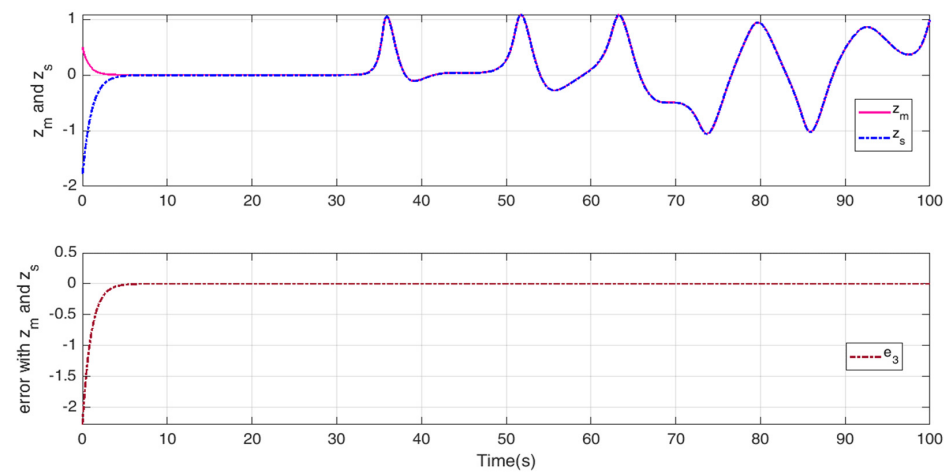


Figure 8. The master–slave synchronization of the third state.

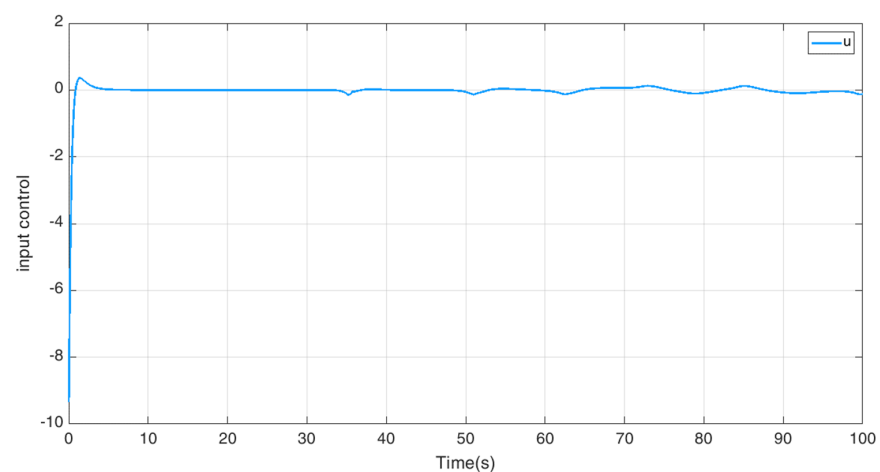


Figure 9. Input control.

As it was observed, synchronization between the master–slave subsystems is performed in a finite timeframe, and synchronization errors converge with very little error near the origin. Thus, we will achieve fast secure communication.

5. Conclusions

In this study, we have presented the complex behaviors of the financial chaotic system in fractional order with two quadratic nonlinearities and a sextic nonlinearity. We validated the existence of chaos via the phase portraits, 0-1 test, Poincaré map, bifurcation diagram, and Lyapunov exponent. The analysis showed that the financial risk chaotic system of fractional order is able to exhibit chaotic behavior and periodical behavior. Finally, an illustrative example was given, and the terminal adaptive finite-time SMC technique was analyzed. The demonstrative examples were discussed to illustrate the efficacy and applicability of the new finite-time control strategy.

Author Contributions: Conceptualization, M.D.J. and A.S.; methodology, S.M.; software, S.M. and B.V.; validation, S.M., B.V. and S.; resources, S.F.A.-A.; investigation, M.D.J.; formal analysis, M.D.J.; data curation, S.; writing—review and editing, M.D.J. and I.M.S.; writing—original draft preparation, A.S., S.M. and I.M.S., visualization, S.F.A.-A. All authors have read and agreed to the published version of the manuscript.

Funding: This research was funded by Universitas Padjadjaran for the project financial support.

Institutional Review Board Statement: Not applicable.

Informed Consent Statement: Not applicable.

Data Availability Statement: Not applicable.

Acknowledgments: The author thanks to Universitas Padjadjaran for financial support.

Conflicts of Interest: The authors state that they have no competing interests.

References

1. Zhuo, P.J.; Zhang, Z.X.; Gou, X.F. Chaotic motion of a magnet levitated over a superconductor. *IEEE Trans. Appl. Supercond.* **2016**, *26*, 1–6. [[CrossRef](#)]
2. Abro, K.A. Numerical study and chaotic oscillations for aerodynamic model of wind turbine via fractal and fractional differential operators. *Numer. Methods Partial. Differ. Equ.* **2022**, *38*, 1180–1194. [[CrossRef](#)]
3. Pappu, C.S.; Carroll, T.L.; Flores, B.C. Simultaneous radar-communication systems using controlled chaos-based frequency modulated waveforms. *IEEE Access* **2020**, *8*, 48361–48375. [[CrossRef](#)]
4. Sambas, A.; Vaidyanathan, S.; Zhang, X.; Koyuncu, I.; Bonny, T.; Tuna, M.; Alcin, M.; Zhang, S.; Sulaiman, I.M.; Awwal, A.M.; et al. A Novel 3D Chaotic System with Line Equilibrium: Multistability, Integral Sliding Mode Control, Electronic Circuit, FPGA and its Image Encryption. *IEEE Access* **2022**, *10*, 68057–68074. [[CrossRef](#)]
5. Mou, J.; Sun, K.; Ruan, J.; He, S. A nonlinear circuit with two memcapacitors. *Nonlinear Dyn.* **2016**, *86*, 1735–1744. [[CrossRef](#)]
6. Naik, R.D.; Singru, P.M. Resonance, stability and chaotic vibration of a quarter-car vehicle model with time-delay feedback. *Commun. Nonlinear Sci. Numer. Simul.* **2011**, *16*, 3397–3410. [[CrossRef](#)]
7. Fakhraei, J.; Khanlo, H.M.; Ghayour, M. Chaotic behaviors of a ground vehicle oscillating system with passengers. *Sci. Iranica. Trans. B Mech. Eng.* **2017**, *24*, 1051. [[CrossRef](#)]
8. Lim, T.S.; Lu, Y.; Nolen, J.H. Quantitative propagation of chaos in a bimolecular chemical reaction-diffusion model. *SIAM J. Math. Anal.* **2020**, *52*, 2098–2133. [[CrossRef](#)]
9. Li, S.; He, Y.; Cao, H. Necessary conditions for complete synchronization of a coupled chaotic Aihara neuron network with electrical synapses. *Int. J. Bifurc. Chaos* **2019**, *29*, 1950063. [[CrossRef](#)]
10. Sambas, A.; Vaidyanathan, S.; Bonny, T.; Zhang, S.; Hidayat, Y.; Gundara, G.; Mamat, M. Mathematical model and FPGA realization of a multi-stable chaotic dynamical system with a closed butterfly-like curve of equilibrium points. *Appl. Sci.* **2021**, *11*, 788. [[CrossRef](#)]
11. Nakamura, Y.; Sekiguchi, A. The chaotic mobile robot. *IEEE Trans. Robot. Autom.* **2001**, *17*, 898–904. [[CrossRef](#)]
12. Atangana, A.; Bonyah, E.; Elsadany, A.A. A fractional order optimal 4D chaotic financial model with Mittag-Leffler law. *Chin. J. Phys.* **2020**, *65*, 38–53. [[CrossRef](#)]
13. Bekiros, S.; Jahanshahi, H.; Munoz-Pacheco, J.M. A new buffering theory of social support and psychological stress. *PLoS one* **2022**, *17*, e0275364. [[CrossRef](#)] [[PubMed](#)]
14. Fanti, L.; Manfredi, P. Chaotic business cycles and fiscal policy: An IS-LM model with distributed tax collection lags. *Chaos Solitons Fractals* **2007**, *32*, 736–744. [[CrossRef](#)]
15. Orlando, G. A discrete mathematical model for chaotic dynamics in economics: Kaldor's model on business cycle. *Math. Comput. Simul.* **2016**, *125*, 83–98. [[CrossRef](#)]
16. Barnett, W.A.; Bella, G.; Ghosh, T.; Mattana, P.; Venturi, B. Shilnikov chaos, low interest rates, and New Keynesian macroeconomics. *J. Econ. Dyn. Control.* **2022**, *134*, 104291. [[CrossRef](#)]

17. Kyrtsov, C.; Labys, W.C. Evidence for chaotic dependence between US inflation and commodity prices. *J. Macroecon.* **2006**, *28*, 256–266. [[CrossRef](#)]
18. Sukono; Sambas, A.; He, S.; Liu, H.; Vaidyanathan, S.; Hidayat, Y.; Saputra, J. Dynamical analysis and adaptive fuzzy control for the fractional-order financial risk chaotic system. *Adv. Differ. Equ.* **2020**, *2020*, 674. [[CrossRef](#)]
19. Munoz-Pacheco, J.M.; Zambrano-Serrano, E.; Volos, C.; Tacha, O.I.; Stouboulos, I.N.; Pham, V.T. A fractional order chaotic system with a 3D grid of variable attractors. *Chaos Solitons Fractals* **2018**, *113*, 69–78. [[CrossRef](#)]
20. Wang, Y.L.; Jahanshahi, H.; Bekiros, S.; Bezzina, F.; Chu, Y.M.; Aly, A.A. Deep recurrent neural networks with finite-time terminal sliding mode control for a chaotic fractional-order financial system with market confidence. *Chaos Solitons Fractals* **2021**, *146*, 110881. [[CrossRef](#)]
21. Chen, W.C. Nonlinear dynamics and chaos in a fractional-order financial system. *Chaos Solitons Fractals* **2008**, *36*, 1305–1314. [[CrossRef](#)]
22. Li, H.L.; Hu, C.; Zhang, L.; Jiang, H.; Cao, J. Complete and finite-time synchronization of fractional-order fuzzy neural networks via nonlinear feedback control. *Fuzzy Sets Syst.* **2022**, *443*, 50–69. [[CrossRef](#)]
23. Li, H.L.; Jiang, H.; Cao, J. Global synchronization of fractional-order quaternion-valued neural networks with leakage and discrete delays. *Neurocomputing* **2020**, *385*, 211–219. [[CrossRef](#)]
24. Wang, S.; He, S.; Yousefpour, A.; Jahanshahi, H.; Repnik, R.; Perc, M. Chaos and complexity in a fractional-order financial system with time delays. *Chaos Solitons Fractals* **2020**, *131*, 109521. [[CrossRef](#)]
25. Pan, I.; Korre, A.; Das, S.; Durucan, S. Chaos suppression in a fractional order financial system using intelligent regrouping PSO based fractional fuzzy control policy in the presence of fractional Gaussian noise. *Nonlinear Dyn.* **2012**, *70*, 2445–2461. [[CrossRef](#)]
26. Wang, Z.; Huang, X.; Zhao, Z. Synchronization of nonidentical chaotic fractional-order systems with different orders of fractional derivatives. *Nonlinear Dyn.* **2012**, *69*, 999–1007. [[CrossRef](#)]
27. Hajipour, A.; Tavakoli, H. Dynamic analysis and adaptive sliding mode controller for a chaotic fractional incommensurate order financial system. *Int. J. Bifurc. Chaos* **2017**, *27*, 1750198. [[CrossRef](#)]
28. Yousri, D.; Mirjalili, S. Fractional-order cuckoo search algorithm for parameter identification of the fractional-order chaotic, chaotic with noise and hyper-chaotic financial systems. *Eng. Appl. Artif. Intell.* **2020**, *92*, 103662. [[CrossRef](#)]
29. Cao, Y. Chaotic synchronization based on fractional order calculus financial system. *Chaos Solitons Fractals* **2020**, *130*, 109410. [[CrossRef](#)]
30. Wang, B.; Liu, J.; Alassafi, M.O.; Alsaadi, F.E.; Jahanshahi, H.; Bekiros, S. Intelligent parameter identification and prediction of variable time fractional derivative and application in a symmetric chaotic financial system. *Chaos Solitons Fractals* **2022**, *154*, 111590. [[CrossRef](#)]
31. Subartini, B.; Vaidyanathan, S.; Sambas, A.; Zhang, S. Multistability in the Finance Chaotic System, Its Bifurcation Analysis and Global Chaos Synchronization via Integral Sliding Mode Control. *IAENG Int. J. Appl. Math.* **2021**, *51*, 995–1002.
32. Xu, X.; Lee, S.D.; Kim, H.S.; You, S.S. Management and optimisation of chaotic supply chain system using adaptive sliding mode control algorithm. *Int. J. Prod. Res.* **2021**, *59*, 2571–2587. [[CrossRef](#)]
33. Yin, C.; Dadras, S.; Zhong, S.M.; Chen, Y. Control of a novel class of fractional-order chaotic systems via adaptive sliding mode control approach. *Appl. Math. Model.* **2013**, *37*, 2469–2483. [[CrossRef](#)]
34. Yan, J.J.; Hung, M.L.; Liao, T.L. Adaptive sliding mode control for synchronization of chaotic gyros with fully unknown parameters. *J. Sound Vib.* **2006**, *298*, 298–306. [[CrossRef](#)]
35. Ghamati, M.; Balochian, S. Design of adaptive sliding mode control for synchronization Genesio–Tesi chaotic system. *Chaos Solitons Fractals* **2015**, *75*, 111–117. [[CrossRef](#)]
36. Mohadeszadeh, M.; Delavari, H. Synchronization of fractional-order hyperchaotic systems based on a new adaptive sliding mode control. *Int. J. Dyn. Control.* **2017**, *5*, 124–134. [[CrossRef](#)]
37. Li, W.L.; Chang, K.M. Robust synchronization of drive–response chaotic systems via adaptive sliding mode control. *Chaos Solitons Fractals* **2009**, *39*, 2086–2092. [[CrossRef](#)]
38. Min, F.; Li, C.; Zhang, L.; Li, C. Initial value-related dynamical analysis of the memristor-based system with reduced dimensions and its chaotic synchronization via adaptive sliding mode control method. *Chin. J. Phys.* **2019**, *58*, 117–131. [[CrossRef](#)]
39. Maeng, G.; Choi, H.H. Adaptive sliding mode control of a chaotic non-smooth-air-gap permanent magnet synchronous motor with uncertainties. *Nonlinear Dyn.* **2013**, *74*, 571–580. [[CrossRef](#)]
40. Khan, A.; Singh, S. Generalization of combination-combination synchronization of n-dimensional time-delay chaotic system via robust adaptive sliding mode control. *Math. Methods Appl. Sci.* **2018**, *41*, 3356–3369. [[CrossRef](#)]
41. Shang, Z.; Yu, Y.; Li, Y. Adaptive sliding mode control of chaotic oscillation in power system based on relay characteristic function. In Proceedings of the 2020 IEEE/IAS Industrial and Commercial Power System Asia (I&CPS Asia), Weihai, China, 13–15 July 2020; pp. 1012–1016.
42. Shukla, V.K.; Vishal, K.; Srivastava, M.; Singh, P.; Singh, H. Multi-switching compound synchronization of different chaotic systems with external disturbances and parametric uncertainties via two approaches. *Int. J. Appl. Comput. Math.* **2022**, *8*, 1–22. [[CrossRef](#)]
43. Aqeel, M.; Ahmad, S.; Azam, A.; Ahmed, F. Dynamical and fractal properties in periodically forced stretch-twist-fold (STF) flow. *Eur. Phys. J. Plus* **2007**, *132*, 1–13. [[CrossRef](#)]

44. Al-Azzawi, S.F. Stability and bifurcation of pan chaotic system by using Routh–Hurwitz and Gardan methods. *Appl. Math. Comput.* **2012**, *219*, 1144–1152. [[CrossRef](#)]
45. Sun, K. *Chaotic Secure Communication: Principles and Technologies*. Tsinghua University Press and Walter de Gruyter GmbH: Beijing, China, 2016; pp. 119–135.
46. Wolf, A.; Swift, J.B.; Swinney, H.L.; Vastano, J.A. Determining Lyapunov exponents from a time series. *Phys. D Nonlinear Phenom.* **1985**, *16*, 285–317. [[CrossRef](#)]

Disclaimer/Publisher’s Note: The statements, opinions and data contained in all publications are solely those of the individual author(s) and contributor(s) and not of MDPI and/or the editor(s). MDPI and/or the editor(s) disclaim responsibility for any injury to people or property resulting from any ideas, methods, instructions or products referred to in the content.